


# The Millennial model: in search of measurable pools and transformations for modeling soil carbon in the new century

Rose Abramoff  · Xiaofeng Xu · Melannie Hartman · Sarah O'Brien ·  
Wenting Feng · Eric Davidson · Adrien Finzi · Daryl Moorhead ·  
Josh Schimel · Margaret Torn · Melanie A. Mayes

Received: 3 August 2017 / Accepted: 10 December 2017 / Published online: 20 December 2017  
© Springer International Publishing AG, part of Springer Nature 2017

**Abstract** Soil organic carbon (SOC) can be defined by measurable chemical and physical pools, such as mineral-associated carbon, carbon physically entrapped in aggregates, dissolved carbon, and fragments of plant detritus. Yet, most soil models use conceptual rather than measurable SOC pools. What would the traditional pool-based soil model look like if it were built today, reflecting the latest understanding of biological, chemical, and physical transformations in soils? We propose a conceptual model—the

Millennial model—that defines pools as measurable entities. First, we discuss relevant pool definitions conceptually and in terms of the measurements that can be used to quantify pool size, formation, and destabilization. Then, we develop a numerical model following the Millennial model conceptual framework to evaluate against the Century model, a widely-used standard for estimating SOC stocks across space and through time. The Millennial model predicts qualitatively similar changes in total SOC in response to single factor perturbations when compared to Century, but different responses to multiple factor perturbations. We review important conceptual and behavioral differences between the Millennial and Century modeling approaches, and the field and lab measurements needed to constrain parameter values. We propose the Millennial model as a simple but comprehensive

---

Responsible Editor: Marc G. Kramer.

---

The submitted manuscript has been authored by contractors of the US Government under contracts DE-AC02-05CH11231 (LBNL), DE-AC02-06CH11357 (ANL), and DE-AC05-00OR22725 (ORNL). Accordingly, the US Government retains a nonexclusive, royalty-free license to publish or reproduce the published form of this contribution, or allow others to do so, for US Government purposes.

---

R. Abramoff (✉) · M. Torn  
Climate and Ecosystem Sciences Division, Lawrence  
Berkeley National Laboratory, 1 Cyclotron Road,  
Berkeley, CA 94720, USA  
e-mail: rzabramoff@lbl.gov

M. Torn  
e-mail: mstorn@lbl.gov

X. Xu  
Biology Department, San Diego State University,  
San Diego, CA 92182, USA  
e-mail: xxu@mail.sdsu.edu

M. Hartman  
Natural Resource Ecology Laboratory, Colorado State  
University, Fort Collins, CO 80523-1499, USA  
e-mail: melannie.hartman@colostate.edu

S. O'Brien  
Biosciences Division, Argonne National Laboratory, 9700  
C Cass Ave., Argonne, IL 60439, USA  
e-mail: slobrien1@gmail.com

framework to model SOC pools and guide measurements for further model development.

**Keywords** Modeling · Soil carbon · Organic matter · Microbial activity · Decomposition · Global change

## Introduction

Changes to inputs or outputs of soil organic carbon (SOC) can affect land carbon (C) storage, and can alter the function of terrestrial ecosystems and their ability to serve as a source or sink of C (Schimel 1995). Researchers use mathematical representations to estimate current distributions and future changes in SOC, incorporating knowledge and assumptions about soil biogeochemical processes. Current earth system models apply soil models that assume first-order kinetic exchanges among conceptual pools defined by empirical turnover times (Todd-Brown et al. 2011, 2013). These models reflected the cutting edge of C cycle science in the 1970s and 1980s (e.g., based on Century and RothC; see review by Manzoni and Porporato 2009). Such models are still of great utility as they capture many essential dynamics, are mathematically simple, and run efficiently over large spatial and temporal scales. However, first-order and empirical representations lack the mechanisms to predict SOC response to global change perturbations such as

centennial-scale warming, drought, priming, and CO<sub>2</sub> or N fertilization (Sierra et al. 2012; Grant 2013; Sulman et al. 2014; Todd-Brown et al. 2014; Zaehle et al. 2014). Further, these models predict divergent SOC stocks under global change scenarios, and do not reproduce current global SOC patterns (Todd-Brown et al. 2013; Wieder et al. 2013). Most earth system models (ESMs) use a soil model consisting of one to three SOC pools (Jenkinson and Coleman 2008; Koven et al. 2013; Luo et al. 2015). Pools in these models are operationally defined based on their presumed chemical composition and turnover times (Parton et al. 1987). Advances in spectroscopy, microscopy, and isotopic labeling, however, have provided a better understanding of the chemical and physical characteristics of SOC (Feng et al. 2016; Chenu and Plante 2006). These new approaches have provided additional evidence that diverse SOC compounds can have similar turnover times (Kleber et al. 2011). As a result, chemical composition is recognized as only one of several factors contributing to the turnover times of SOC pools (Schmidt et al. 2011). Other factors protecting SOC from decomposition include the physical structure of soil and chemical associations with soil minerals (von Lützow et al. 2007; Cotrufo et al. 2013; Lehmann and Kleber 2015). Recent studies have called for a new generation of soil biogeochemical models that better represent the chemical and physical mechanisms controlling SOC

---

### *Present Address:*

S. O'Brien  
Department of Biological Sciences, University of Illinois at Chicago, 845 W Taylor St. MC 066, Chicago, IL 60607, USA

W. Feng  
Department of Microbiology and Plant Biology,  
University of Oklahoma, 101 David L. Boren, Norman,  
OK 73019, USA  
e-mail: wenting.fwt@gmail.com

E. Davidson  
Appalachian Laboratory, University of Maryland Center  
for Environmental Science, 301 Braddock Road,  
Frostburg, MD 21529, USA  
e-mail: edavidson@umces.edu

A. Finzi  
Department of Biology and PhD Program in  
Biogeoscience, Boston University, 5 Cummington St,  
Boston, MA 02215, USA  
e-mail: afinzi@bu.edu

D. Moorhead  
Department of Environmental Sciences, University of  
Toledo, 2801 W Bancroft, St. Toledo, OH 43606, USA  
e-mail: daryl.moorhead@utoledo.edu

J. Schimel  
Department of Ecology, Evolution and Marine Biology,  
University of California Santa Barbara, 1108 Noble Hall,  
Santa Barbara, CA 93106, USA  
e-mail: schimel@lifesci.ucsb.edu

M. A. Mayes  
Environmental Science Division & Climate Change  
Science Institute, Oak Ridge National Laboratory,  
P.O. Box 2008, Oak Ridge, TN 37830, USA  
e-mail: mayesma@ornl.gov

turnover (Schmidt et al. 2011; Todd-Brown et al. 2013; Luo et al. 2015; Wieder et al. 2015a, b).

A growing number of soil models consider an explicit microbial biomass pool that affects the decomposition rate of SOC (Schimel and Weintraub 2003; Allison et al. 2010; German et al. 2012). These models often require greater numbers of parameters and equations, but may have an improved ability to predict responses to novel environmental conditions, e.g., global change scenarios (Wieder et al. 2013; Hararuk et al. 2013). Questions remain about the feasibility of applying microbial models to global SOC predictions (Bradford et al. 2016). Nevertheless, it is timely to rethink how we model key soil processes in light of new emphasis on the nature of SOC and decomposition pathways.

If we were to start over and develop a mathematical model for SOC based on current understanding of soil C pools, it would reflect the biological, chemical, and physical knowledge of soils gained in the last decades. The model would classify organic C into categories defined by measurable chemical and physical properties, such as mineral-associated C, C physically entrapped in aggregates, dissolved C, and fragments of plant detritus. A model based on measurable pools would represent explicit processes regulating the transfers of C between pools, in contrast to models based on imposed turnover times. For example, if SOC is occluded within aggregates, the processes that determine whether C is decomposed to CO<sub>2</sub>, preserved, or transformed include those that regulate aggregate turnover such as slaking, freeze–thaw, and tillage. In this approach, the factors that cause aggregate formation and destruction would be simulated to the extent possible, rather than simply assigning the C within aggregates as part of a pool defined by a conceptually- or empirically-derived first-order decay constant. Thus, starting with measurable pools and transformations of SOC would allow us to define the rate-limiting processes for each pool and to build a model that incorporates an expanded suite of the most important driving processes in soil—biological, chemical, and physical.

### The Millennial model

Herein we describe a conceptual model that retains the tractability of Century but is more directly

testable because it is based on measurable soil pools. We then develop a numerical model (Appendix) following the Millennial conceptual model, and evaluate this model against the Century model to illustrate potential differences between the two model structures. Last, we discuss what measurements are needed to constrain the Millennial model and the empirical challenges related to those measurements.

### Definitions of SOC pools for the Millennial model

The Millennial model has five measurable soil C pools: particulate organic matter (i.e., free fragments of plant detritus; POM), low molecular weight C (i.e., root exudates and the by-products of exoenzyme activity; LMWC), aggregate C, mineral-associated organic matter (MAOM), and microbial biomass carbon (Fig. 1). In the following section, we define each pool conceptually and in terms of the measurements that can be used to quantify pool size, formation, and destabilization.

#### *Particulate organic matter*

POM is material that retains identifiable characteristics of its source material. POM is derived primarily from plant material, but also from dead insects, fungi, and detritus generated through fragmentation and decomposition of litter, and from breakup of pre-existing soil aggregates (Segoli et al. 2013; Cotrufo et al. 2015). POM can be measured using an operationally-defined size and/or density separation (Six et al. 2006; Six and Paustian 2014). POM may become associated with soil aggregates, but is broadly defined by limited association with soil minerals. POM can be chemically altered by microbial activity, leaching, and UV exposure (Baker and Allison 2015).

#### *Low molecular weight carbon*

LMWC refers to generally mono- or oligomeric, soluble products of microbial decomposition and plant inputs such as root exudates and leaf leachate. LMWC concentrations measured by an elemental analyzer are typically higher in surface soil horizons, but preferential flow from biological activity (e.g., rooting and invertebrate activity), physical forces (e.g., erosion, cracks, and fractures formed by freeze–thaw), leaching (advection), or management practices (e.g.,

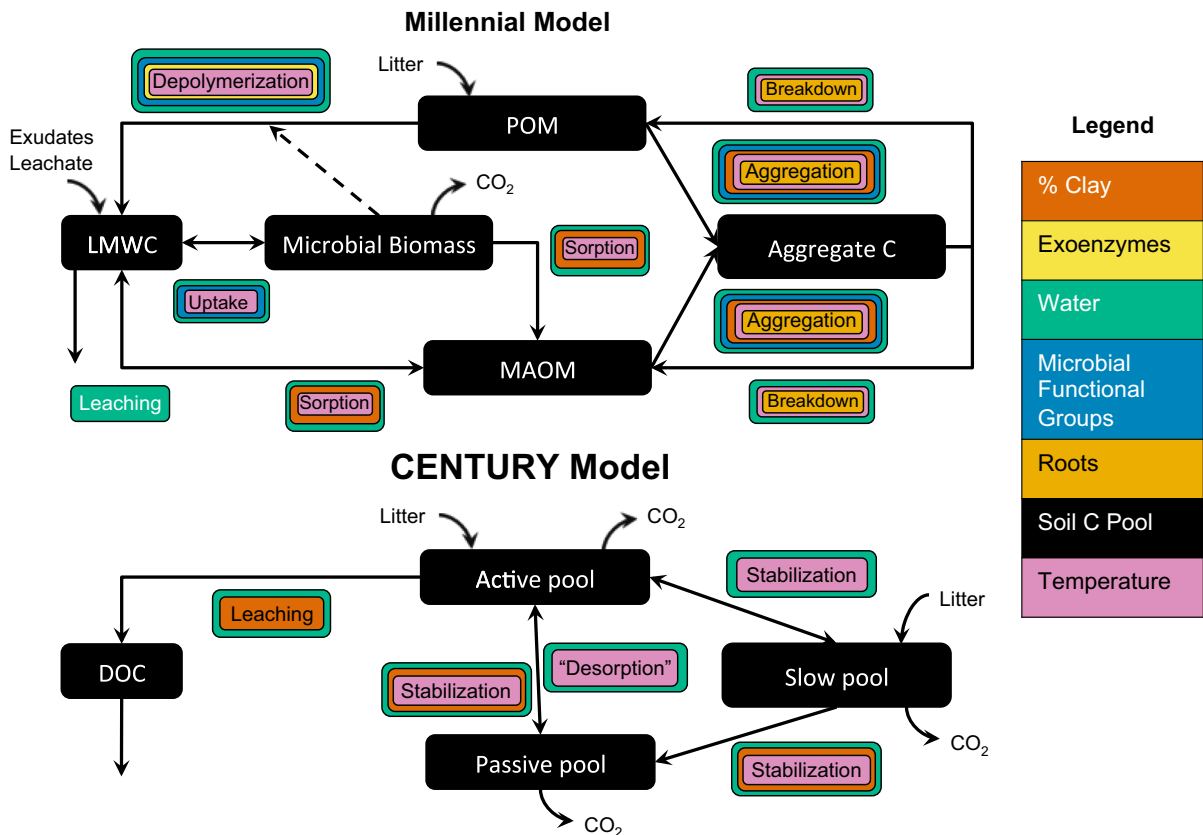


**Fig. 1** Conceptual model diagram of the Millennial (top) and Century models (bottom). The black boxes are carbon pools, and the colored boxes are fluxes. Solid arrows indicate the direction of each flux. The color legend indicates edaphic, biological, and

climatic factors that may modify the rate of a given flux. Dash lines indicate controls (i.e., microbial biomass regulates the depolymerization rate)

plowing) may enable vertical transport (Gerke 2006; Boddy et al. 2007). LMWC can be removed from solution during transport by becoming adsorbed to soil minerals or consumed by microbes (Kaiser and Kalbitz 2012; Jardine et al. 2006). The pore structure of soils, however, may limit microbial and enzyme access to LMWC (Young and Crawford 2004; Zhuang et al. 2008; Smith et al. 2017). Sorption of LMWC can vary according to its functional groups (Jagadamma et al. 2012).

### Aggregate C

We define soil aggregates as three-dimensional arrangements of organic matter and minerals where the forces holding them together are stronger than the forces attracting them to other aggregates (Martin et al. 1955). Aggregate structures form when

microbial residues and organic binding agents attract soil particles, often in the presence of structural support and chemical residues provided by plant roots and fungal hyphae (Jastrow et al. 1998; Young and Crawford 2004). Aggregates range in size from silt-sized objects < 20  $\mu\text{m}$  to microaggregates (53–2000  $\mu\text{m}$ ) to large macroaggregates (2000–8000  $\mu\text{m}$ ) (Plante et al. 2006; Virto et al. 2008). These operationally-defined size classes can exist in a hierarchical network (e.g., microaggregates within macroaggregates) in the soil, and tend to be more stable as size decreases and layers of protection increase (Tisdall and Oades 1982; Dexter 1988). SOC in aggregates can be protected from decomposition when the pore network limits diffusion of gases or nutrients (Sexstone et al. 1985; Horn et al. 1994; Ranjard and Richaume 2001; Young et al. 2008), isolates substrates from extracellular enzymes (Mayer

1994; Ekschmitt et al. 2005; Allison 2006; Allison and Jastrow 2006), or limits access of grazing organisms (Mayer 1994; Ranjard and Richaume 2001). Aggregate formation and disruption occurs as a natural part of soil formation and carbon cycling, whereby physical or chemical processes (e.g., drying, wetting, freeze–thaw, tillage, electrostatic interactions) interact with biological mechanisms (e.g., microbial exudation, root and hyphal entanglement) to build and destabilize aggregates over time (Six et al. 2000; Deneff et al. 2002; Pronk et al. 2012).

#### *Mineral-associated organic matter*

MAOM is protected from microbial decomposition (and transport) through a variety of sorption mechanisms, such as surface complexation, cation bridging, and hydrophobic interactions (Sollins et al. 1996; Kaiser et al. 1996; Kleber et al. 2007; Torn et al. 2009). MAOM typically refers to the heavy mineral soil fraction isolated by density fractionations or the fine soil particles measured by size fractionation. Across a wide variety of soil types and geographical locations, MAOM accounts for a large proportion (50–85%) of the total SOC stock in bulk soil (Sollins et al. 2009; Marin-Spiotta et al. 2009; Heckman et al. 2014; Cai et al. 2016), and in most soils SOC in MAOM has a longer mean turnover time than other measurable soil fractions such as aggregates and POM (Feng et al. 2016; Marin-Spiotta et al. 2009; Jagadamma et al. 2013; Torn et al. 1997).

The formation of MAOM is regulated by adsorption of compounds such as LMWC and microbially-derived products to mineral surfaces (Kalbitz and Kaiser 2008; Lehmann and Kleber 2015). Microbially-derived products may be preferentially adsorbed onto soil minerals compared to other compounds (Sollins et al. 2009; Rumpel et al. 2010; Cotrufo et al. 2015). Layering of organic compounds on soil minerals may also impart protection (Wershaw 1986; Kleber et al. 2007). Factors that influence the formation and stability of MAOM include OM chemistry, soil texture, structure, the physico-chemical properties and abundance of soil minerals, pH, the ionic strength of soil water, temperature, and moisture (Jardine and McCarthy 1989; Kothawala et al. 2009; Mayes et al. 2012; Feng et al. 2015).

#### *Microbial biomass*

Microbial biomass herein is defined as the mass of C contained within soil microbial cells. Microbial biomass can be estimated using a variety of methods, such as substrate-induced respiration, chloroform fumigation, phospholipid fatty acid analysis, and quantitative PCR (Anderson and Domsch 1978; Vance et al. 1987; Bååth and Anderson 2003; Junicke et al. 2014). Microbial biomass controls the flow of C in soils through uptake of C and nutrients for microbial growth, the release of waste products, and microbial turnover. Specifically, microbes produce extracellular enzymes to decompose SOC, and they release CO<sub>2</sub> through maintenance and growth respiration (Schmidt et al. 2011). Necromass can be transferred to LMWC, aggregate C, and MAOM pools (Cotrufo et al. 2013; Kallenbach et al. 2016). Given the significantly different turnover rates of these carbon pools, the relative fraction of these allocations could determine how long necromass C will remain in the soil.

Microbial biomass is not a large pool, typically < 5% of SOC (Fahey et al. 2005; Fontaine et al. 2007; Abramoff and Finzi 2016), but microbial activity has a disproportionate effect on C cycling. As such, microbial activity largely controls the SOC response to global change. Global change is proposed to affect microbial functions in a number of ways. Particularly, soil warming may (1) increase the activity of microbial predators, (2) alter the proportion of C taken up that is allocated to growth [carbon use efficiency (CUE)], (3) shift microbial community composition, (4) accelerate protein turnover, and (5) increase microbial metabolic activity (Steinweg et al. 2008; Frey et al. 2013; DeAngelis et al. 2015). Beyond soil temperature, other factors that may affect growth rates and turnover times include the size of microbial biomass, soil moisture, soil texture, microbial biomass C:N:P ratio, soil pH, and supply of substrates such as litter, root turnover, root exudates, and SOC (Grant 2001; Manzoni et al. 2014; Sinsabaugh et al. 2014b; Tang and Riley 2015).

#### Major differences between the Millennium and Century models

The Century model has been a standard for estimating soil C stocks across space and through time for three decades (Parton et al. 1987, 1995; Paustian et al. 1992;

Bonan et al. 2013). For this reason, we compare the conceptual organization of the Millennial model to that of the Century model. The Century and Millennial models both transfer C between several solid-phase C pools and a LMWC pool, modifying rates of transfer based on edaphic and climatic factors. The ‘active’ pool in Century represents material with short turnover times (6 months–1 year) and is often conceptualized as live microbial biomass and microbial products, the ‘slow’ pool is defined by having an intermediate turnover time (10–50 years) and is thought to be chemically-resistant or physically-protected, and the ‘passive’ pool, with the longest turnover time (100–1000 years), is considered chemically or physically-stabilized (e.g., charcoal or bound to clay particles). The transfer of C between pools is controlled by constant maximum specific decay rates that can be set to site-specific values. Turnover rates are then empirically modified by environmental factors (e.g., temperature, moisture, pH, aeration) and soil physical properties (e.g., sand, silt, and clay content). Implicitly, Century considers SOC to be stabilized by physico-chemical interactions such as humification and adsorption to clay particles. The result is a direct transfer of C from the active or slow pools to the passive pool. The proportion of C allocated to the passive pool from the active pool compared to the slow pool has increased over time, reflecting accumulating evidence (e.g., Cotrufo et al. 2013, 2015) of the role of microbes and labile C in forming protected C. Dissolved organic C (DOC) in Century is formed as a linear function of sand content and the amount of water flowing through the organic horizon, but it cannot be stabilized and eventually leaches out of the system.

In the Millennial model, the soil pools—POM, LMWC, aggregate C, MAOM, and microbial biomass—are based on measurable components of SOC, and transfers between pools are conceptualized as transfers that would occur in nature. For example, C transfers between pools do not result in CO<sub>2</sub> loss unless they are mediated by microbial activity. POM can become associated with aggregate C, or transformed into LMWC by microbial biomass. LMWC can be taken up by microbial biomass and transformed to CO<sub>2</sub>, sorbed to minerals or leached away. LMWC and microbial necromass are the main sources of C in MAOM. Rather than a linear transfer from POM to aggregate C to MAOM, both POM and MAOM can

reversibly bind to aggregate C. Because microbes mediate or transfer mass between all of the C pools, we would expect this model to have several significant differences in dynamics, and the potential to generate a wider range of feedbacks in responses to climate perturbations, when compared to a first-order model.

Several recent models have explicitly represented the microbial decomposition of soil organic matter. These models all have different approaches to microbial decomposition and soil C protection. For example, a model by Wang et al. (2013) used the Michaelis–Menten equation, with enzymes produced by an explicit pool of microorganisms, to estimate production of DOC from both POM and MAOM, while allowing the latter to dynamically sorb to soil minerals. Ahrens et al. (2015) also used a saturating sorption isotherm, but used microbial biomass instead of enzyme concentration to simulate decomposition and predict the vertical age profile of SOM. A third model by Tang and Riley (2015) used equilibrium approximation kinetics to represent both enzymatic decomposition and sorption to minerals, while Dwivedi et al. (2017) used a surface complexation model to estimate sorption. Other models do not use sorption to minerals but represent soil C cycling in new ways. For example, Wieder et al. (2015a, b) introduced microbial functional groups to constrain the decomposition rates of two litter and soil pools, while Sistla et al. (2014) included multiple substrate and enzyme functional groups. Sulman et al. (2014) tracked three substrate pools (simple, chemically resistant, and dead microbes) allocated between protected and unprotected fractions. In this model, decay rate was a saturating function of the microbe:substrate ratio, and protected SOM was a composite of aggregate C and MAOM.

None of the models above explicitly simulated soil aggregates or aggregate C. In contrast, Segoli et al. (2013) explicitly simulated soil aggregate dynamics, hierarchically nesting four size classes. Aggregation was driven by litter decomposition and microbial production, albeit with first-order kinetics and omitting other soil organic matter pools. To our knowledge, no existing model matches our conceptualization of the pools both necessary and minimally sufficient to meet the emerging consensus on biological, chemical, and physical controls on SOC, though the key pools and fluxes are well represented across recent models when considered

together. The Millennial model expands on these recently developed models not by including all of their features, but by focusing on the processes that control our five C pools, such as microbial decomposition, mineral sorption, and aggregation.

## Model comparison

We developed a numerical model following the Millennial model conceptual framework to illustrate potential behaviors of such a model structure. We describe the five C pools of the Millennial model and the rate of transfer between them in a series of ordinary differential equations defined in the Appendix. To illustrate key conceptual and structural differences between the Millennial model and the Century model, we compared predicted SOC stocks using both models across a gradient of clay content and in response to global change scenarios. We used the same parameter values for both models when possible (Table 3), and adjusted a subset of parameters (Table 3, “Calibrated”) in the Millennial model to better match the steady-state SOC stocks predicted by the Century model. The purpose of this fitting was to perturb both models from a similar initial condition in order to focus on the different perturbation responses between the two models. We ran the Millennial model and Century for 2000 years after an initial spin-up of 4000 years, using identical soil temperature, moisture, and plant inputs (Table 1). The soil temperature and moisture forcing was a global average derived from the Community ESM (Oleson et al. 2013). The carbon input is representative of mid-high latitudes. All input files are available at <https://github.com/email-clm/Millennial>, along with the model code. One year of input forcing was repeated for the number of years of

the model simulation. The initial soil C in each of the five soil C pools was set to  $1 \text{ g m}^{-2}$  prior to spin-up. In the first set of scenarios, we compared steady-state C pools in soils with different clay content (10, 20, 30, 40, 50, 60, 70, 80%), reflecting a gradient in the sorption capacity of soil. Second, we compared the equilibrium size of soil C pools after 2000 years following temperature, moisture, and substrate perturbations. The initial values for the soil C pools in the perturbation scenarios were derived from the end of the 4000-year spin-up scenario at 40% clay. We chose the following perturbations to represent common global change scenarios (Melillo et al. 2011; Suseela et al. 2012; Lajtha et al. 2014a) used for model sensitivity analysis (Sierra et al. 2015; Wang et al. 2016), 5 °C warming (W), double C input (I), 50% of the original soil moisture content (D), 5 °C warming and double C input (WI), and 5 °C warming and 50% soil moisture (WD).

## Comparison of Millennial and Century model runs

### Sensitivity to clay content

The Millennial and Century models had similar amounts of C in analogous pools. The majority of C in the Millennial model at steady state was in the MAOM pool, similar to Century’s passive pool (Fig. 2a, b). Aggregate C in the Millennial model was 14–20% of total SOC, similar to Century’s slow pool. In the Millennial model, LMWC, microbial biomass, and POM represented < 6% of total C, similar to the active pool in Century. In the simulations, a greater proportion of C inputs were stabilized as MAOM in the 80% clay compared to the 20% clay soil, because of the larger sorption capacity of the 80% clay soil.

**Table 1** Input information for Millennial and Century model runs

|  | Control | W    | I    | D    | WI   | WD   |
|--|---------|------|------|------|------|------|
| Mean annual soil temperature (°C)                            | 11.2    | 16.2 | 11.2 | 11.2 | 16.2 | 16.2 |
| Mean annual volumetric SWC ( $\text{mm}^3 \text{ mm}^{-3}$ ) | 0.24    | 0.24 | 0.24 | 0.12 | 0.24 | 0.12 |
| Litter inputs ( $\text{g C m}^{-2} \text{ year}^{-1}$ )      | 172     | 172  | 344  | 172  | 344  | 172  |

SWC soil water content, W 5 °C warming, I double C input, D half water, WI warming and double C input, WD warming and half water

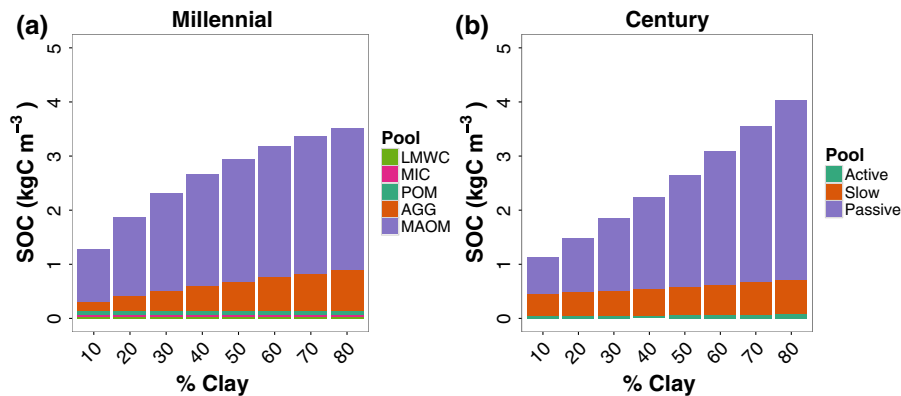


**Fig. 2** Bar chart of the Millennial (a) and Century (b) model predictions of soil organic carbon (SOC) as a function of clay content. *LMWC* low molecular weight C, *MIC* microbial

biomass, *POM* particulate organic matter, *AGG* aggregate C, *MAOM* mineral-associated organic matter

There were, however, several differences between the Millennial and Century model outputs. First, the Millennial model uses nonlinear functions based on experiments to predict the relationship between the maximum sorption capacity ( $Q_{\max}$ ) and clay content, imposing maximum carbon storage capacity in the MAOM pool (Mayes et al. 2012; Wang et al. 2013; Riley et al. 2014; Ahrens et al. 2015; Dwivedi et al. 2017), whereas in Century, the C stored in each pool changes proportionally with forcings such as clay content and plant inputs. As a result, SOC approaches a maximum value as soil clay content increased in the Millennial model (Fig. 2a) whereas the size of these pools increased proportionally with clay content in the Century model (Fig. 2b). Second, the Millennial model reached an equilibrium C stock more quickly than did Century (Fig. 3a, b). This reflects the faster transfer of C inputs to the dominant SOC pool (MAOM) in the Millennial model than to the dominant pool (passive C) in Century.

#### *Response to single factor climate and environmental forcings*

The models made different SOC predictions in single factor climate and environmental forcing simulations (Figs. 4a, b, 5a, b). Century accumulated more C in response to doubled input than did the Millennial model. Georgiou et al. (2017) demonstrated that soil C accumulation in a first-order model was proportional to plant inputs, but a microbial model was insensitive to plant inputs because of the concomitant increase in

microbial growth and respiration that removes some of the added plant inputs via respiration. This feedback between plant inputs and biomass growth may explain why increased C input has a smaller effect on SOC pools in the Millennial model compared with the Century model. The Millennial results are consistent with experiments which demonstrate that increased plant inputs and SOC responses are not linearly related (Lajtha et al. 2014a, b). It is notable that some of the added C remained in the POM pool rather than becoming incorporated into a physically or chemically protected pool, making it theoretically more vulnerable to remineralization.

Warming by 5 °C decreased SOC in both models (Fig. 4a, b). The temperature sensitivity of decomposition in the Millennial model is greater than in the Century model and thus it lost more SOC in response to the warming perturbation (Fig. 4a). The Millennial model uses the same scalar for temperature sensitivity as Century, but also uses a temperature-sensitive microbial CUE (Table 3) that increases the respiratory loss of SOC with warming.

Both models gained SOC with a 50% decrease in field moisture content (Fig. 4a, b). The Millennial model gained more SOC than the Century model compared to the control treatment (Figs. 4, 5). The Millennial model may be somewhat more sensitive to drought because the water scalar affects multiple microbial processes such as decomposition and uptake, as well as physical processes such as sorption and aggregate formation. Neither model is coupled to a model of plant productivity; thus, feedback effects



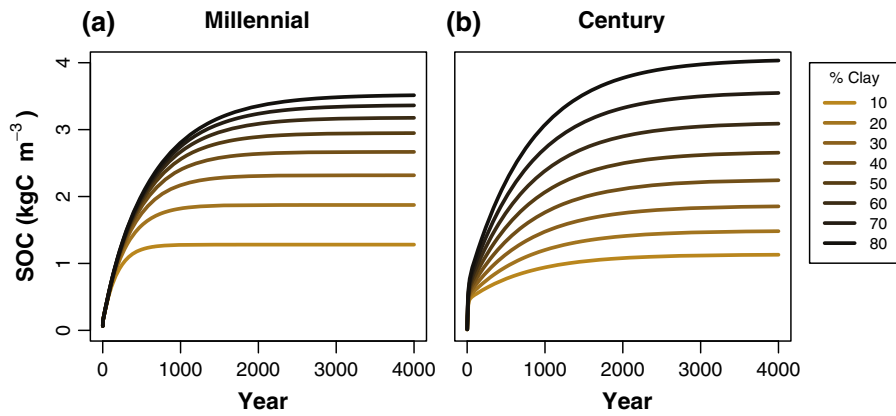


**Fig. 3** Time series of the Millennial (a) and Century (b) model predictions of total soil organic carbon (SOC) with varying clay content from initialization to 4000 years

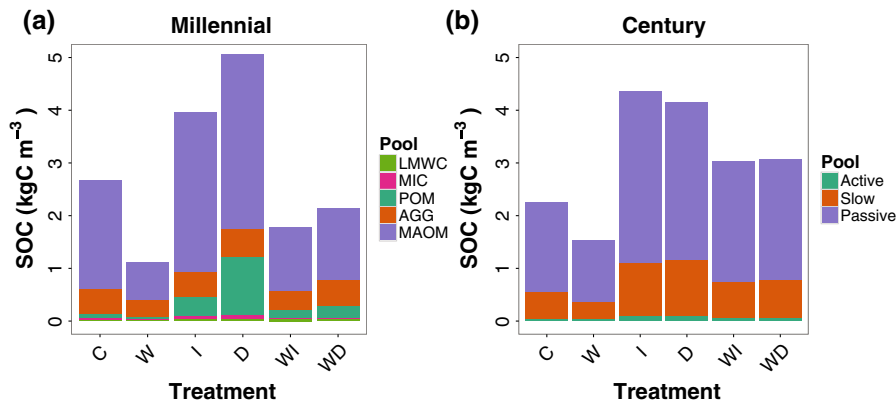


**Fig. 4** Bar chart of the Millennial (a) and Century (b) model predictions of soil organic carbon (SOC) following 2000 years of a perturbation to temperature, moisture, plant inputs, or a combination. *W* 5 °C warming, *I* double C input, *D* half water, *WI* warming and double C input, *WD* warming and half water, *LMWC* low molecular weight C, *MIC* microbial biomass, *POM* particulate organic matter, *AGG* aggregate C, *MAOM* mineral-associated organic matter

*WI* warming and double C input, *WD* warming and half water, *LMWC* low molecular weight C, *MIC* microbial biomass, *POM* particulate organic matter, *AGG* aggregate C, *MAOM* mineral-associated organic matter

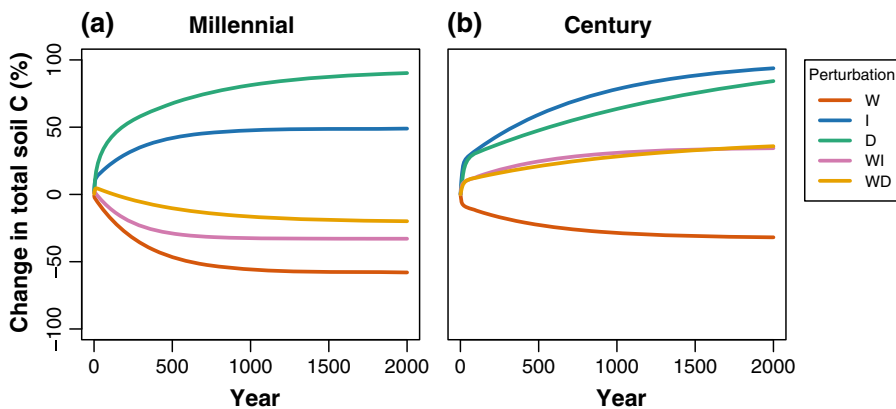


**Fig. 5** Time series of the Millennial (a) and Century (b) model predictions of the change in total soil carbon (C) relative to the control following a sustained change to temperature, moisture, plant inputs, or a combination for 2000 years. *W* 5 °C warming, *I* double C input, *D* half water, *WI* warming and double C input, *WD* warming and half water

plant inputs, or a combination for 2000 years. *W* 5 °C warming, *I* double C input, *D* half water, *WI* warming and double C input, *WD* warming and half water

on SOC simulated here only reflect soil processes. Given the sensitivity of SOC to plant inputs in the Century model, it is likely that the negative effect of drought on plant productivity would reduce SOC. In the Millennial model, this effect may be dampened because plant inputs are less important to SOC concentrations than are the internal biophysical processes (e.g., microbial growth, enzyme production, sorption).

### *Response to dual-factor climate and environmental forcings*

In contrast to the single-factor perturbations, the interaction of warming with double-litter inputs or drought resulted in fundamentally different SOC responses in the two models. When warming was coupled with double inputs or decreases in soil moisture, the Millennial model lost SOC relative to the control simulations, whereas the Century model gained SOC compared to the control. In Century, doubled plant inputs and drought strongly increased SOC, while warming moderately decreased SOC—thus, the strong effect of plant inputs and soil moisture resulted in a net SOC increase (Figs. 4, 5). In the Millennial model, warming had the strongest effect, ultimately decreasing SOC to a greater extent than the positive effect on SOC of plant inputs and drought. It is notable that the two models had the same sign of change in SOC stock with regards to single-factor variation in clay content, temperature, soil moisture, and double inputs. Yet, when simultaneous perturbations were applied, the direction of the SOC trend diverged. The unique features of the Millennial model—the use of a temperature-sensitive CUE, and nonlinear responses to increases in plant inputs—are likely responsible for the different responses compared to Century. We cannot say which model simulation was most accurate, and in fact, the answer is likely dependent on local edaphic conditions. Few large-scale field manipulations have been able to test more than one forcing factor (Norby and Luo 2004; Castro et al. 2010; Hanson et al. 2016). But the divergence observed here clearly demonstrates the sensitivity of future predictions of the SOC sink to different model formulations (e.g., Todd-Brown et al. 2013).

### What are the costs of process-rich models?

Including measurable SOC pools in the Millennial model adds realism to C fluxes and transformations, while increasing flexibility to respond to climate and environmental forcing factors. However, this added realism has costs. For example, replacing the empirical equations in Century with the more mechanistic ones in the Millennial model increases the number of model equations and parameters. The additional costs may be partly offset by defining pools and fluxes that are potentially measurable, thus providing empirical constraints to at least some of the additional parameters that can be measured (but see section below on measurement challenges).

Any formulation of the Millennial model including the one we present above, is more complex than Century, and requires more knowledge to develop equations and define parameters. For example, the microbial pool is explicitly used to estimate POM decay, LMWC assimilation, respiration, and MAOM sorption, requiring kinetic parameters instead of the simpler rate coefficients used in Century. Estimates of these parameters in our numerical model (Table 3) were derived from studies completed since Century was developed, or were calibrated to constrain model behaviors within reported bounds. Including additional processes, or developing existing processes to be more mechanistic, would similarly require more equations, parameters, and constraints.

No model can capture every biological process, and the Millennial model omits some important controls. For example, decomposition is constrained by both energetic and stoichiometric relationships between microorganisms and nutrients (Sinsabaugh and Shah 2012), but we have only considered C in the Millennial model. Including only C can increase model sensitivity to parameters affecting carbon flow that would realistically be constrained by other nutrients. Moreover, many model parameters are not constants, but variables that change in ways that could dampen model responses. A good example is CUE. Including temperature-dependent CUE can result in large differences in SOC predictions after warming compared to fixed-CUE models (Wang et al. 2013; Wieder et al. 2013). Yet the relationship between temperature and CUE used in this and other models is based on few studies (Devêvre and Horváth 2000; van Ginkel et al. 2000; Steinweg et al. 2008), and relationships between

CUE and other attributes of the environment, resources, and microbial community are areas of active research (Geyer et al. 2016; Sinsabaugh et al. 2017).

Although the Millennial model is necessarily more mechanistic than Century in calculating flows between pools of soil C, it remains empirical with regard to underlying biochemical and physiological processes. For example, microbial biomass is a surrogate, in part, for the actions of extracellular enzymes catalyzing substrate degradation (Burns et al. 2013). Adding specific classes of extracellular enzymes to the Millennial model would provide context to more mechanistically evaluate the influence of substrate quality or nutrient availability on patterns of C flow (Moorhead et al. 2012; Averill 2014). It would also add several equations describing dynamics of additional pools, require many parameters, and the need to balance enzyme production, turnover, and activity with comparable substrate and microbial dynamics (Sinsabaugh et al. 2014a, b).

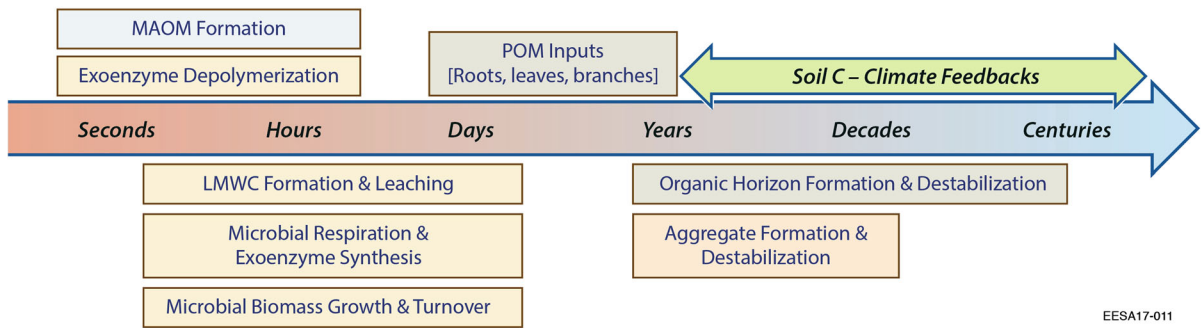
The desired temporal and spatial scale of model predictions and scale of model formulation can guide the necessary level of mechanistic representation. Adapting models for problems at different scales also requires consideration of mathematical complexity, parameter choice, and feedback control. Some processes such as microbial growth and enzymatic depolymerization operate on sub-hourly-to-daily timescales. While these short-term processes may be important for long-term trends, it may be computationally intractable to represent these processes in models that run over timescales of decades to centuries (Fig. 6). Further, it may not be necessary to represent these processes if they can be seasonally averaged or otherwise collapsed into relationships between responses and their drivers, creating a simplified model of response variables related to empirical observations (Todd-Brown et al. 2011). For example, Xu et al. (2014) derived an index of cumulative microbial activity from readily available climate data that was then used in conjunction with substrate C:N to estimate the ratio of microbial biomass C to substrate C for locations where microbial biomass observations were not available. Wieder et al. (2013) used Michaelis–Menten kinetics to model decay rate as a function of microbial biomass, which could be estimated according to Xu et al. (2014), to generate soil C pools closer to observations than predictions

from Century-based models (DAYCENT and CLM4CN; Thornton et al. 2007). These examples demonstrate how fine-scale microbial models can be used to generate scalable relationships between easily observed variables (e.g., soil C:N) and key model parameters (e.g., microbial biomass) for use in ESMs. Thus one of the practical advantages of developing new fine-scale microbial models is the transfer of knowledge from a modern representation of decomposition to large spatial and temporal scales via their application in an ESM. Of course, the transfer must retain sufficient mechanistic representation such that the ESM makes reasonable projections under novel environmental conditions.

### Measurability of pools

The Millennial model represents a hypothesis about what biological, chemical, and physical soil processes are important to C cycling. Exploring this hypothesis through simulations can provide guidance for prioritizing measurements of soil pools, transfer rates, and environmental factors. Models currently use a wide variety of data for fitting and validation, including microbial biomass measurements from laboratory incubations (Wang et al. 2013), litter decomposition and soil C pool measurements (Wieder et al. 2014, 2015a, b), total soil C and protected C (Sulman et al. 2014), laboratory measurements of aggregate C (Segoli et al. 2013), and field measurements of heterotrophic respiration (Abramoff et al. 2017). Estimates of soil C pools and factors affecting them such as litter decomposition, heterotrophic respiration, and clay content can be measured in the field either directly or by proxy (Bailey et al. 2017; Table 2). However, the Millennial model also requires new parameters governing process equations that are challenging to measure, especially regarding aggregate dynamics and MAOM. These processes have only been considered in a handful of models due to a lack of observational data (Albalasmeh and Ghezzehei 2013; Segoli et al. 2013; Wang et al. 2013; Ahrens et al. 2015; Tang and Riley 2015).

It is relatively straightforward to quantify the proportion of soil mass or soil C in aggregates, but it is far more challenging to estimate the rate of aggregate formation and decay (Table 2). Most studies measure the turnover of the carbon in aggregates at



EESA17-011

**Fig. 6** Conceptual diagram of time scales over which particular soil processes occur, from seconds to centuries. *Soil C-climate feedbacks* effects of changes to soil processes on greenhouse gas

concentrations in the atmosphere, *MAOM* mineral-associated organic matter, *POM* particulate organic matter, *LMWC* low molecular weight carbon

**Table 2** Measurability of factors influencing pools

| Soil C pool | Widely measured          | Measurable by proxy   | Mechanisms that need proxies and/or other data to define rate constants  |
|-------------|--------------------------|---|--|
| Aggregate C | Clay content<br>Rainfall | Root exudation<br>Fungal production<br>Aggregate/aggregate-C turnover<br>Root growth                  | Bioturbation<br>Plowing<br>Compaction<br>Freeze–thaw<br>Effect of rainfall on aggregates<br>Necromass production |
| MAOM        | pH                       | Organic content on mineral surface<br>Mineralogy<br>$\text{PO}_4^{3-}/\text{SO}_4^{2-}$ concentration | Tillage<br>Oxidative enzymes<br>Electrostatic interactions<br>Ionic strength<br>Necromass production             |
| POM         | NPP                      | Secondary production<br>Litter chemistry<br>Decomposition of litter                                   | Fragmentation of litter  |
| LMWC        | Soil moisture            | DOC concentration<br>Leaching rate  | Sorption potential   |
| Microbes    | Soil temperature         | Microbial biomass<br>Microbial growth rate<br>Respiration<br>CUE<br>Enzyme activity                   | Internal allocation<br>Fate of necromass<br>Competition  |

the time of sampling rather than the turnover of the physical structure of the aggregates themselves (e.g., Jastrow et al. 1996; Six et al. 1998; Liao et al. 2006). Carbon dynamics can be decoupled from the turnover rates of the physical structures (O'Brien and Jastrow 2013; McCarthy et al. 2008) and there can be a large

range of SOC ages within a single aggregate or group of aggregates, leading to dramatic overestimation of aggregate turnover times (Jastrow et al. 1996). Approaches for estimating aggregate turnover that are independent of soil C such as labeling with rare earth elements, controlled laboratory studies, or

observation after disturbance in the field tend to find shorter turnover times, but the results also depend on the time interval of observation (De Gryze et al. 2006) or experimental treatment (O'Brien and Jastrow 2013; Deneff et al. 2002; Crawford et al. 2012; Blankinship et al. 2016) making it difficult to generalize. Therefore, aggregate C parameters are the most uncertain of the Millennial model parameters, though the physically-based definition of aggregates makes them potentially measurable.

MAOM is difficult to measure consistently because there is no standard fractionation procedure, either in terms of pre-treatment of samples or threshold values for solution density and soil particle size. Different methods estimate widely diverging turnover times for MAOM, ranging from  $24 \pm 7$  years using incubations,  $166 \pm 44$  years using  $^{13}\text{C}$  labeling, and  $709 \pm 121$  years using  $^{14}\text{C}$  labeling (Feng et al. 2016). Studies that define MAOM using a density fraction tend to estimate longer turnover times (e.g., 30–4500 years; Heckman et al. 2014; Hall et al. 2015) than studies that estimate MAOM using a size fraction (e.g., 18–665 and 24–1280 years for the silt and clay size fractions, respectively; O'Brien et al. 2013). Given the potential value of the Millennial model and the importance of the turnover times of modeled pools, we contend that research effort should be directed toward robust assays and protocols that will provide consistent estimates of aggregate and MAOM turnover time in the field.

## Conclusion

We developed a soil modeling framework that reflects current understanding about the biological, chemical, and physical mechanisms controlling the formation and destabilization of soil carbon and is based on the principle of measurable model pools. This framework emphasizes how limited access of microbial decomposers to soil C imparts stability to SOC, in contrast to the Century model which defines decomposition rates empirically as a function of environmental factors. We created a numerical model based on this framework and identified areas of consistency with the Century model, including similar predictions of SOC as a function of clay content, temperature, soil moisture, and plant inputs. Because the Century model is the standard by which other models are judged, we are

encouraged by the observed consistency. However, the Millennial model exhibited distinct nonlinear responses due to the choice of functions affecting SOC in the soil pools, e.g., the Michaelis–Menten equation for depolymerization, and the sorption equation for stabilization of LMWC on MAOM. More importantly, the two models diverged regarding the direction of SOC stock change (sink vs. source) when more than one environmental or climate forcing factor was imposed at the same time. It is uncertain whether the Millennial or Century formulation is more consistent with observations, but the variation in model behavior points to the importance of understanding underlying pool transformations.

While the accuracy of the Millennial model is untested, it is our intent that the underlying modeling framework represents the current conceptual understanding of soil C, and therefore has the potential to be developed into a model that skillfully represents a variety of global change processes, including climate and land use change. The mechanistic C transformations enable predictions of SOC under novel environmental conditions, and measurable pools make the model more testable in theory. In practice, the model demonstrates the need for field and laboratory measurements of rates of aggregate and mineral-associated C formation and decay. Nevertheless, we propose that the Millennial model offers a new, independent path for improving understanding and predictions of soil responses to anthropogenic, environmental, and climatic forcing factors by representing measurable soil C pools and transfer processes in a transparent and parsimonious model structure.

**Acknowledgements** The Millennial model code, model inputs, and the model output used in this manuscript are archived at a GITHUB Repository (<https://github.com/email-clm/Millennial>) that is publicly accessible. The authors would like to thank the Carbon Cycle Interagency Working Group, via the US Carbon Cycle Science Program under the auspices of the US Global Change Research Program, for providing funding for the “Celebrating the 2015 International Decade of Soil – Understanding Soil’s Resilience and Vulnerability,” workshop held at the University Corporation for Atmospheric Research in Boulder, CO, USA on 14–16 March 2016. We would also like to thank the University Corporation for Atmospheric Research for providing meeting space, as well as the 36 workshop participants, William J. Riley, and three anonymous reviewers for helpful comments and discussion. Lawrence Berkeley National Laboratory is managed and operated by the Regents of the University of California under Contract DE-AC02-05CH11231 with the US Department of Energy. Argonne National

Laboratory is managed by UChicago Argonne, LLC, under contract DE-AC02-06CH11357 with the US Department of Energy. Oak Ridge National Laboratory is managed by the University of Tennessee-Battelle, LLC, under Contract DE-AC05-00OR22725 with the US Department of Energy.

### Compliance with ethical standards

**Conflict of Interest** The authors declare that they have no conflict of interest.

### Appendix: Model description

The equations we have chosen below reflect one possible mathematical expression of the Millennial conceptual model, but there are many possible numerical models for different applications. For example, decomposition of POM is here represented by a double Monod relationship, limited by both POM and microbial biomass, but for an application where competition between chemical species is particularly important, for example, ECA kinetics could be used instead (Tang 2015). Similarly, we chose temperature and moisture scalars to minimize steady-state differences between Millennial and Century for the purpose of model comparison, but for dynamic predictions one could apply Arrhenius temperature sensitivity and one of several semi-mechanistic moisture functions (Davidson et al. 2012; Manzoni et al. 2014).

The system of equations below is modeled on the conceptual figure (Fig. 1), tracking the size of and transfers between five C pools: POM, LMWC, aggregate C, MAOM, and microbial biomass. The change in POM ( $P$ ) stock with time is governed by the balance between plant C input and aggregate C breakdown, aggregate C formation, and decomposition,

$$dP/dt = p_i F_i + p_a F_a - F_{pa} - F_{pl}, \quad (1)$$

where  $F_i$  is aboveground plant litter, root litter and root exudates,  $p_i$  is the proportion of C input allocated to POM (1/3 of inputs to POM and 2/3 of inputs to LMWC after Oleson et al. 2013),  $p_a$  is the proportion of C in aggregate breakdown allocated to POM,  $F_a$  is aggregate C breakdown,  $F_{pa}$  is aggregate carbon formation from POM, and  $F_{pl}$  is decomposition of POM into LMWC. Decomposition of POM is governed by a double Michaelis–Menten equation,

$$F_{pl} = V_{pl} \frac{P}{K_{pl} + P} \frac{B}{K_{pe} + B} S_t S_w, \quad (2)$$

where  $V_{pl}$  is the maximum rate of POM decomposition,  $K_{pl}$  is the half-saturation constant,  $B$  is the microbial biomass carbon, and  $K_{pe}$  is the half-saturation constant of microbial control on POM mineralization. The terms  $S_t$  and  $S_w$  refer to the temperature and moisture scalar, respectively, and are taken from DAYCENT, the daily time-step version of the Century model (Parton et al. 1998), to minimize differences in temperature and moisture effects between the Century and Millennial models due to choice of scalar,

$$S_t = \left( \frac{t_2 + (t_3/pi) \operatorname{atan}(pi(T - t_1))}{t_2 + (t_3/pi) \operatorname{atan}(pi t_4 (T_{ref} - t_1))} \right), \quad (3)$$

$$S_w = \frac{1}{1 + w_1 \exp(-w_2 RWC)}, \quad (4)$$

where  $T$  is the current temperature,  $T_{ref}$  is the reference temperature,  $t_1$  is the x-axis location of the inflection point ( $^{\circ}\text{C}$ ),  $t_2$  is the y-axis location of the inflection point,  $t_3$  is the distance from the maximum point to the minimum point, and  $t_4$  is the slope of the line at the inflection point. For the water scalar,  $RWC$  is the relative water content calculated as the fraction of field capacity, and  $w_1$  and  $w_2$  are empirical parameters. The temperature scalar is an arctangent function that predicts a decline in temperature sensitivity with increasing temperature and the water scalar depends on RWC, where the maximum effect on biological activity occurs at field capacity (volumetric water content = 0.35, RWC = 1.0) (Parton et al. 2010).

The formation of aggregate C (A) from POM follows Michaelis–Menten dynamics,

$$F_{pa} = \frac{V_{pa} P}{K_{pa} + P} \left( 1 - \frac{A}{A_{max}} \right) S_t S_w, \quad (5)$$

where  $V_{pa}$  is the maximum rate of aggregate formation,  $K_{pa}$  is the half-saturation constant of aggregate formation, and  $A_{max}$  is the maximum capacity of C in soil aggregates. Soil aggregate C breakdown is partitioned to POM and MAOM,

$$F_a = k_b S_t S_w A, \quad (6)$$

where  $k_b$  is the rate of breakdown.

The change in LMWC ( $L$ ) depends on LMWC input, the leaching rate, decomposition of POM, adsorption to minerals, and microbial uptake. In a

multilayer version of the Millennial model LMWC would also depend on leaching input, but in this single layer version we assume that the leaching input is included in the LMWC input,

$$dL/dt = F_i(1 - p_i) - F_l + F_{pl} - F_{lm} - F_{lb}, \quad (7)$$

where  $F_l$  is the LMWC leaching loss,

$$F_l = k_l S_t S_w L \quad (8)$$

and where  $k_l$  is the leaching rate,  $F_{lm}$  is the adsorption of LMWC to MAOM, and  $F_{lb}$  is the uptake of LMWC by microbial biomass. Adsorption of LMWC to minerals is controlled by a Langmuir saturation function,

$$F_{lm} = S_t S_w L \left( \frac{K_{lm} Q_{max} L}{1 + (K_{lm} L)} - M \right) / Q_{max}, \quad (9)$$

$$K_{lm} = 10^{(-0.186pH - 0.216)}, \quad (10)$$

$$Q_{max} = BD 10^{(c_1 \log(\%clay) + c_2)}, \quad (11)$$

where  $K_{lm}$  is the binding affinity that is adjustable based on the pH.  $Q_{max}$  is the maximum sorption capacity (mg C kg<sup>-1</sup> dry soil) that is converted to C density (g C m<sup>-2</sup>) by multiplying soil bulk density ( $BD = 1350$  kg m<sup>-3</sup>), assuming a 1 m soil profile. The parameters  $c_1$  and  $c_2$  are the coefficients for computing  $Q_{max}$  from the clay content in percent, derived from Mayes et al. (2012). The Langmuir function parameters were derived from measurements of DOC sorption on over 200 soils in the eastern US. The measurements demonstrate a nonlinear saturation with respect to DOC concentrations in soils, and several recent models have used approaches that also impose a mechanism for DOC saturation on mineral surfaces (Wang et al. 2013; Riley et al. 2014; Ahrens et al. 2015; Dwivedi et al. 2017).

Microbial uptake of LMWC is a function of microbial biomass and LMWC concentration, temperature, water, and temperature-dependent CUE,

$$F_{lb} = V_{lm} S_t S_w L \frac{B}{B + K_{lb}} (CUE_{ref} - CUE_T (T - T_{ae-ref})), \quad (12)$$

$$F_{gr} = V_{lm} S_t S_w L \frac{B}{B + K_{lb}} (1 - (CUE_{ref} - CUE_T (T - T_{ae-ref}))), \quad (13)$$

where  $V_{lm}$  is the potential uptake rate of LMWC.  $F_{gr}$  is microbial growth-related respiration,  $K_{lb}$  is the half-saturation constant for microbial activity,  $CUE_{ref}$  is the reference CUE, and  $CUE_T$  is the CUE dependence on temperature.  $T_{ae-ref}$  and  $T$  are the reference and current temperature, respectively. Both MAOM and POM can be incorporated into the aggregate C pool,

$$dA/dt = F_{ma} + F_{pa} - F_a, \quad (14)$$

$$F_{ma} = \frac{V_{ma} M}{K_{ma} + M} \left( 1 - \frac{A}{A_{max}} \right) S_t S_w, \quad (15)$$

where  $F_{ma}$  is the carbon flow from MAOM to aggregate C,  $V_{ma}$  is the maximum rate of aggregate formation, and  $K_{ma}$  is the half-saturation constant of aggregate formation. MAOM is formed by adsorption of LMWC and microbial necromass, and is affected by transfer into and out of the aggregate C pool,

$$dM/dt = F_{lm} + F_{bm} - F_{ma} + F_a (1 - p_a), \quad (16)$$

$$F_{bm} = k_{mm} S_t S_w B, \quad (17)$$

where  $F_{bm}$  is the carbon flow from microbial biomass to MAOM, namely adsorption of necromass, and  $k_{mm}$  is the adsorption rate of microbial biomass. In this particular iteration of the Millennial model, we assume that adsorbed microbial biomass is no longer alive, but by allowing adsorbed microbial biomass to take up LMWC and perform growth and maintenance, one could modify the model to accommodate the assumption that live microbial biomass can sorb to minerals, or even to other microbes (i.e., biofilms). Microbial biomass changes as a result of uptake, adsorption to minerals, and loss via maintenance,

$$dB/dt = F_{lb} - F_{bm} - F_{mr}, \quad (18)$$

$$F_{mr} = k_m S_t S_w B, \quad (19)$$

where  $F_{mr}$  is the maintenance respiration of microbial biomass, and  $k_m$  is the microbial turnover rate (Table 3).

**Table 3** Parameters, pools, fluxes and other variables used in the Millennial model

| Eq.    | Variables    | Definitions  | Ranges/values and units                         | Sources                                   |
|--------|--------------|--|---|---|
| 1, 7   | $p_i$        | Proportion of C input allocated to POM                               | 2/3 (unitless)                                  | Oleson et al. (2013)                      |
| 1, 16  | $p_a$        | Proportion of aggregate-C breakdown allocated to POM                 | 1/3 (unitless)                                  | Oleson et al. (2013)                      |
| 2      | $V_{pt}$     | Maximum rate of POM decomposition to LMWC                            | 10 (g C m <sup>-2</sup> day <sup>-1</sup> )     | Calibrated                                |
| 2      | $K_{pt}$     | Half-saturation constant of POM decomposition to LMWC                | 150 (g C m <sup>-2</sup> day <sup>-1</sup> )    | Calibrated                                |
| 2      | $K_{pe}$     | Half saturation constant for microbial control on POM mineralization | 12 (g C m <sup>-2</sup> )                       | Calibrated                                |
| 3      | $T_{ref}$    | Reference temperature for the temperature scalar                     | 30 (°C)   | Del Grosso et al. (2005)                  |
| 3      | $t_1$        | x-axis location of inflection point                                  | 15.4 (°C)                                       | Del Grosso et al. (2005)                  |
| 3      | $t_2$        | y-axis location of inflection point                                  | 11.75   | Del Grosso et al. (2005)                  |
| 3      | $t_3$        | Distance from the maximum point to the minimum point (step size)     | 29.7  | Del Grosso et al. (2005)                  |
| 3      | $t_4$        | Slope of line at inflection point                                    | 0.031   | Del Grosso et al. (2005)                  |
| 4      | $w_1$        | Water scalar parameter   | 30 (unitless)                                   | Parton et al. (2010)                      |
| 4      | $w_2$        | Water scalar parameter   | 9 (unitless)                                    | Parton et al. (2010)                      |
| 5      | $V_{pa}$     | Maximum rate of aggregate formation from POM                         | 0.002 (gC m <sup>-2</sup> day <sup>-1</sup> )   | Calibrated                                |
| 5      | $K_{pa}$     | Half-saturation constant of aggregate formation from POM             | 50 (g C m <sup>-2</sup> )                       | Calibrated                                |
| 5, 15  | $A_{max}$    | Maximum capacity of soil aggregate carbon                            | 500 (g C m <sup>-2</sup> )                      | Calibrated                                |
| 6      | $k_b$        | Breakdown rate of soil aggregate carbon                              | 0.0002 (unitless)                               | Calibrated                                |
| 8      | $k_l$        | Leaching rate of LMWC  | 0.0015 (g C m <sup>-2</sup> day <sup>-1</sup> ) | Calibrated                                |
| 9, 10  | $K_{lm}$     | Binding affinity for LMWC sorption                                   | 0.25 (g C m <sup>-2</sup> )                     | Calibrated                                |
| 10     | $pH$         | pH   | 7 (unitless)                                    | Mayes et al. (2012)                       |
| 11     | $c_1$        | Coefficient for estimating the maximum sorption capacity             | 0.297 (unitless)                                | Mayes et al. (2012)                       |
| 11     | $c_2$        | Coefficient for estimating the maximum sorption capacity             | 3.355 (unitless)                                | Mayes et al. (2012)                       |
| 11     | $BD$         | Bulk density   | 1350 (kg m <sup>-3</sup> )                      | Mayes et al. (2012)                       |
| 12, 13 | $V_{lm}$     | Potential LMWC turnover rate   | 0.35 (g C m <sup>-2</sup> day <sup>-1</sup> )   | Calibrated                                |
| 12, 13 | $K_{lb}$     | Half saturation constant for microbial activity                      | 7.2 (g C m <sup>-2</sup> )                      | Schimel and Weintraub (2003)              |
| 12, 13 | $CUE_{ref}$  | Reference CUE  | 0.6 (unitless)                                  | Xu et al. (2014)                          |
| 12, 13 | $CUE_T$      | CUE dependence on temperature  | - 0.012 (degree <sup>-1</sup> )                 | Xu et al. (2014)                          |
| 12, 13 | $T_{ae-ref}$ | Reference temperature for temperature control on CUE                 | 15 (°C)   | Xu et al. (2014)                          |
| 15     | $V_{ma}$     | Maximum rate of aggregate formation from MAOM                        | 0.07 (g C m <sup>-2</sup> day <sup>-1</sup> )   | Calibrated                                |
| 15     | $K_{ma}$     | Half-saturation constant for aggregate formation from MAOM           | 200 (g C m <sup>-2</sup> )                      | Calibrated                                |
| 17     | $k_{mm}$     | Microbial biomass adsorption rate                                    | 0.025 (unitless)                                | Calibrated                                |
| 19     | $k_m$        | Microbial turnover rate  | 0.036 (day <sup>-1</sup> )                      | Wieder et al. (2013) and Xu et al. (2014) |



**Table 3** continued

| Eq.                                  | Variables | Definitions   | Ranges/values and units | Sources    |
|--------------------------------------|-----------|---|-------------------------|------------|
| 1, 2, 5                              | $P$       | POM   |                         | Calculated |
| 7–9, 12, 13                          | $L$       | LMWC  |                         | Calculated |
| 2, 12, 13, 17–19                     | $B$       | Microbial biomass   |                         | Calculated |
| 9, 15, 16                            | $M$       | MAOM  |                         | Calculated |
| 5, 6, 14, 15                         | $A$       | Aggregate C   |                         | Calculated |
| 1, 7                                 | $F_i$     | C input   |                         | Calculated |
| 1, 6, 14, 16                         | $F_a$     | Aggregate breakdown   |                         | Calculated |
| 1, 5, 14                             | $F_{pa}$  | Aggregate formation from POM                                      |                         | Calculated |
| 1, 2, 7                              | $F_{pt}$  | Decomposition of POM into LMWC                                    |                         | Calculated |
| 2, 3, 5, 6, 8, 9, 12, 13, 15, 17, 19 | $s_t$     | Temperature scalar  |                         | Calculated |
| 2, 4–6, 8, 9, 12, 13, 15, 17, 19     | $s_w$     | Water scalar  |                         | Calculated |
| 4                                    | $RWC$     | Relative water content  |                         | Calculated |
| 7, 8                                 | $F_l$     | LMWC leaching loss  |                         | Calculated |
| 7, 9, 16                             | $F_{lm}$  | Adsorption of LMWC to minerals                                    |                         | Calculated |
| 7, 12, 18                            | $F_{lb}$  | Uptake of LMWC by microbial biomass                               |                         | Calculated |
| 9, 11                                | $Q_{max}$ | Maximum sorption capacity   |                         | Calculated |
| 11                                   | $\%clay$  | Percent of soil that is in the clay fraction (default value = 40) |                         | Calculated |
| 13                                   | $F_{gr}$  | Microbial growth respiration                                      |                         | Calculated |
| 14–16                                | $F_{ma}$  | Aggregate formation from MAOM                                     |                         | Calculated |
| 16–18                                | $F_{bm}$  | Adsorption of microbial necromass to MAOM                         |                         | Calculated |
| 18, 19                               | $F_{mr}$  | Microbial maintenance respiration                                 |                         | Calculated |

“Calibrated” parameters were adjusted to ensure the total carbon is consistent with the Century model predictions. “Calculated” variables are pools or fluxes whose values are a function of parameters, initial values, and time

Eq. equation number

## References

- Abramoff RZ, Finzi AC (2016) Seasonality and partitioning of root allocation to rhizosphere soils in a midlatitude forest. *Ecosphere*. <https://doi.org/10.1002/ecs2.1547>
- Abramoff RZ, Davidson EA, Finzi AC (2017) A parsimonious modular approach to building a mechanistic belowground carbon and nitrogen model. *J Geophys Res Biogeosci* 122:2418–2434
- Ahrens B, Braakhekke MC, Guggenberger G et al (2015) Contribution of sorption, DOC transport and microbial interactions to the  $^{14}\text{C}$  age of a soil organic carbon profile: insights from a calibrated process model. *Soil Biol Biochem* 88:390–402
- Albalasmeh AA, Ghezzehei TA (2013) Interplay between soil drying and root exudation in rhizosphere development. *Plant Soil* 374:739–751
- Allison SD (2006) Soil minerals and humic acids alter enzyme stability: implications for ecosystem processes. *Biogeochemistry* 81:361–373
- Allison SD, Jastrow JD (2006) Activities of extracellular enzymes in physically isolated fractions of restored grassland soils. *Soil Biol Biochem* 38:3245–3256
- Allison SD, Wallenstein MD, Bradford MA (2010) Soil-carbon response to warming dependent on microbial physiology. *Nat Geosci* 3:336–340
- Anderson JPE, Domsch KH (1978) A physiological method for the quantitative measurement of microbial biomass in soils. *Soil Biol Biochem* 10:215–221

- Averill C (2014) Divergence in plant and microbial allocation strategies explains continental patterns in microbial allocation and biogeochemical fluxes. *Ecol Lett*. <https://doi.org/10.1111/ele.12324>
- Bååth E, Anderson TH (2003) Comparison of soil fungal/bacterial ratios in a pH gradient using physiological and PLFA-based techniques. *Soil Biol Biochem* 35:955–963
- Bailey VL, Bond-Lamberty B, DeAngelis K et al (2017) Soil carbon cycling proxies: understanding their critical role in predicting climate change feedbacks. *Glob Change Biol* 00:1–11
- Baker NR, Allison SD (2015) Ultraviolet photodegradation facilitates microbial litter decomposition in a Mediterranean climate. *Ecology* 96:1994–2003
- Blankinship JC, Fonte SJ, Six J, Schimel JP (2016) Plant versus microbial controls on soil aggregate stability in a seasonally dry ecosystem. *Geoderma* 272:39–50
- Boddy E, Hill P, Farrar J, Jones D (2007) Fast turnover of low molecular weight components of the dissolved organic carbon pool of temperate grassland field soils. *Soil Biol Biochem* 39:827–835
- Bonan GB, Hartman MD, Parton WJ, Wieder WR (2013) Evaluating litter decomposition in earth system models with long-term litterbag experiments: an example using the Community Land Model version 4 (CLM4). *Glob Change Biol* 19:957–974
- Bradford MA, Wieder WR, Bonan GB et al (2016) Managing uncertainty in soil carbon feedbacks to climate change. *Nat Clim Change* 6:751–758
- Burns RG, DeForest JL, Marxsen J et al (2013) Soil enzymes in a changing environment: current knowledge and future directions. *Soil Biol Biochem* 58:216–234
- Cai A, Feng W, Zhang W, Xu M (2016) Climate, soil texture, and soil types affect the contributions of fine-fraction-stabilized carbon to total soil organic carbon in different land uses across China. *J Environ Manag* 172:2–9
- Castro HF, Classen AT, Austin EE et al (2010) Soil microbial community responses to multiple experimental climate change drivers. *Appl Environ Microbiol* 76:999–1007
- Chenu C, Plante AF (2006) Clay-sized organo-mineral complexes in a cultivation chronosequence: revisiting the concept of the “primary organo-mineral complex”. *Eur J Soil Sci* 57:596–607
- Cotrufo MF, Wallenstein MD, Boot CM et al (2013) The Microbial Efficiency-Matrix Stabilization (MEMS) framework integrates plant litter decomposition with soil organic matter stabilization: do labile plant inputs form stable soil organic matter? *Glob Change Biol* 19:988–995
- Cotrufo MF, Soong JL, Horton AJ et al (2015) Formation of soil organic matter via biochemical and physical pathways of litter mass loss. *Nat Geosci* 8:776–779
- Crawford JW, Deacon L, Grinev D et al (2012) Microbial diversity affects self-organization of the soil–microbe system with consequences for function. *J R Soc Interface* 9:1302–1310
- Davidson EA, Samanta S, Caramori SS, Savage K (2012) The Dual Arrhenius and Michaelis–Menten kinetics model for decomposition of soil organic matter at hourly to seasonal time scales. *Glob Change Biol* 18:371–384
- De Gryze S, Six J, Merckx R (2006) Quantifying water-stable soil aggregate turnover and its implication for soil organic matter dynamics in a model study. *Eur J Soil Sci* 57:693–707
- DeAngelis KM, Pold G, Topçuoğlu BD et al (2015) Long-term forest soil warming alters microbial communities in temperate forest soils. *Front Microbiol* 6:104
- Del Grosso SJ, Parton WJ, Mosier AR et al (2005) Modeling soil CO<sub>2</sub> emissions from ecosystems. *Biogeochemistry* 73:71–91
- Denef K, Six J, Merckx R, Paustian K (2002) Short-term effects of biological and physical forces on aggregate formation in soils with different clay mineralogy. *Plant Soil* 246:185–200
- Devèvre OC, Horváth WR (2000) Decomposition of rice straw and microbial carbon use efficiency under different soil temperatures and moistures. *Soil Biol Biochem* 32:1773–1785
- Dexter AR (1988) Advances in characterization of soil structure. *Soil Tillage Res* 11:199–238
- Dwivedi D, Riley WJ, Torn MS, et al (2017) Mineral properties, microbes, transport, and plant-input profiles control vertical distribution and age of soil carbon stocks. *Soil Biol Biochem* 107:244–259
- Ekschmitt K, Liu M, Vetter S et al (2005) Strategies used by soil biota to overcome soil organic matter stability—why is dead organic matter left over in the soil? *Geoderma* 128:167–176
- Fahey TJ, Siccama TG, Driscoll CT et al (2005) The biogeochemistry of carbon at Hubbard Brook. *Biogeochemistry* 75:109–176
- Feng W, Klaminder J, Boily J-F (2015) Thermal stability of goethite-bound natural organic matter is impacted by carbon loading. *J Phys Chem A* 119:12790–12796
- Feng W, Shi Z, Jiang J et al (2016) Methodological uncertainty in estimating carbon turnover times of soil fractions. *Soil Biol Biochem* 100:118–124
- Fontaine S, Barot S, Barré P et al (2007) Stability of organic carbon in deep soil layers controlled by fresh carbon supply. *Nature* 450:277–280
- Frey SD, Lee J, Melillo JM, Six J (2013) The temperature response of soil microbial efficiency and its feedback to climate. *Nat Clim Change* 3:395–398
- Georgiou K, Abramoff RZ, Harte J et al (2017) Microbial community-level regulation explains soil carbon responses to long-term litter manipulations. *Nat Commun* 8:1223
- Gerke HH (2006) Preferential flow descriptions for structured soils. *Z Pflanzenernähr Bodenkd* 169:382–400
- German DP, Marcelo KRB, Stone MM, Allison SD (2012) The Michaelis–Menten kinetics of soil extracellular enzymes in response to temperature: a cross-latitudinal study. *Glob Change Biol* 18:1468–1479
- Geyer KM, Kyker-Snowman E, Grandy AS, Frey SD (2016) Microbial carbon use efficiency: accounting for population, community, and ecosystem-scale controls over the fate of metabolized organic matter. *Biogeochemistry* 127:173–188
- Grant RF (2001) A review of Canadian ecosystem model—ecosys. In: *Modeling carbon and nitrogen dynamics for soil management*, p 173–264. <https://doi.org/10.1201/9781420032635.ch6>
- Grant RF (2013) Modelling changes in nitrogen cycling to sustain increases in forest productivity under elevated

- atmospheric CO<sub>2</sub> and contrasting site conditions. *Biogeosciences* 10:7703–7721
- Hall SJ, McNicol G, Natake T, Silver WL (2015) Large fluxes and rapid turnover of mineral-associated carbon across topographic gradients in a humid tropical forest: insights from paired <sup>14</sup>C analysis. *Biogeosciences* 12:2471–2487
- Hanson PJ, Gill AL, Xu X et al (2016) Intermediate-scale community-level flux of CO<sub>2</sub> and CH<sub>4</sub> in a Minnesota peatland: putting the SPRUCE project in a global context. *Biogeochemistry* 129:255–272
- Hararuk O, Obrist D, Luo Y (2013) Modelling the sensitivity of soil mercury storage to climate-induced changes in soil carbon pools. *Biogeosciences* 10:2393–2407
- Heckman K, Throckmorton H, Clingensmith C et al (2014) Factors affecting the molecular structure and mean residence time of occluded organics in a lithosequence of soils under ponderosa pine. *Soil Biol Biochem* 77:1–11
- Horn R, Taubner H, Wuttke M, Baumgartl T (1994) Soil physical properties related to soil structure. *Soil Tillage Res* 30:187–216
- Jagadamma S, Mayes MA, Phillips JR (2012) Selective sorption of dissolved organic carbon compounds by temperate soils. *PLoS ONE*. <https://doi.org/10.1371/journal.pone.0050434>
- Jagadamma S, Megan Steinweg J, Mayes MA et al (2013) Decomposition of added and native organic carbon from physically separated fractions of diverse soils. *Biol Fertil Soils* 50:613–621
- Jardine PM, McCarthy JF (1989) Mechanisms of dissolved organic carbon adsorption on soil. <https://doi.org/10.2136/sssaj1989.03615995005300050013x>
- Jardine PM, Mayes MA, Mulholland PJ et al (2006) Vadose zone flow and transport of dissolved organic carbon at multiple scales in humid regimes. *Vadose Zone J* 5:140–152
- Jastrow JD, Miller RM, Boutton TW (1996) Carbon dynamics of aggregate-associated organic matter estimated by carbon-13 natural abundance. *Soil Sci Soc Am J* 60:801
- Jastrow JD, Miller RM, Lussenhop J (1998) Contributions of interacting biological mechanisms to soil aggregate stabilization in restored prairie. *Soil Biol Biochem* 30:905–916
- Jenkinson DS, Coleman K (2008) The turnover of organic carbon in subsoils. Part 2. Modelling carbon turnover. *Eur J Soil Sci* 59:400–413
- Junicke H, Abbas B, Oentoro J et al (2014) Absolute quantification of individual biomass concentrations in a methanogenic coculture. *AMB Express*. <https://doi.org/10.1186/s13568-014-0035-x>
- Kaiser K, Kalbitz K (2012) Cycling downwards—dissolved organic matter in soils. *Soil Biol Biochem* 52:29–32
- Kaiser K, Guggenberger G, Zech W (1996) Sorption of DOM and DOM fractions to forest soils. *Geoderma* 74:281–303
- Kalbitz K, Kaiser K (2008) Contribution of dissolved organic matter to carbon storage in forest mineral soils. *Z Pflanzenernähr Bodenkd* 171:52–60
- Kallenbach CM, Frey SD, Grandy AS (2016) Direct evidence for microbial-derived soil organic matter formation and its ecophysiological controls. *Nat Commun* 7:13630
- Kleber M, Sollins P, Sutton R (2007) A conceptual model of organo-mineral interactions in soils: self-assembly of organic molecular fragments into zonal structures on mineral surfaces. *Biogeochemistry* 85:9–24
- Kleber M, Nico PS, Plante A et al (2011) Old and stable soil organic matter is not necessarily chemically recalcitrant: implications for modeling concepts and temperature sensitivity. *Glob Change Biol* 17:1097–1107
- Kothawala DN, Moore TR, Hendershot WH (2009) Soil properties controlling the adsorption of dissolved organic carbon to mineral soils. *Soil Sci Soc Am J* 73:1831–1842
- Koven CD, Riley WJ, Subin ZM et al (2013) The effect of vertically resolved soil biogeochemistry and alternate soil C and N models on C dynamics of CLM4. *Biogeosciences* 10:7109–7131
- Lajtha K, Bowden RD, Nadelhoffer K (2014a) Twenty years of litter and root manipulations in a temperate deciduous forest: Insights into soil organic matter dynamics and stability. *Soil Sci Soc Am J* 78:261–269
- Lajtha K, Townsend KL, Kramer MG et al (2014b) Changes to particulate versus mineral-associated soil carbon after 50 years of litter manipulation in forest and prairie experimental ecosystems. *Biogeochemistry* 119:341–360
- Lehmann J, Kleber M (2015) The contentious nature of soil organic matter. *Nature* 528:60–68
- Liao JD, Boutton TW, Jastrow JD (2006) Storage and dynamics of carbon and nitrogen in soil physical fractions following woody plant invasion of grassland. *Soil Biol Biochem* 38:3184–3196
- Luo Y, Ahlström A, Allison SD et al (2015) Towards more realistic projections of soil carbon dynamics by earth system models. *Glob Biogeochem Cycles*. <https://doi.org/10.1002/2015gb005239>
- Manzoni S, Porporato A (2009) Soil carbon and nitrogen mineralization: theory and models across scales. *Soil Biol Biochem* 41:1355–1379
- Manzoni S, Schaeffer SM, Katul G et al (2014) A theoretical analysis of microbial eco-physiological and diffusion limitations to carbon cycling in drying soils. *Soil Biol Biochem* 73:69–83
- Marin-Spiotta E, Silver WL, Swanston CW, Ostertag R (2009) Soil organic matter dynamics during 80 years of reforestation of tropical pastures. *Glob Change Biol* 15:1584–1597
- Martin JP, Martin WP, Page JB et al (1955) Soil aggregation. *Adv Agron* 7:1–37
- Mayer LM (1994) Relationships between mineral surfaces and organic carbon concentrations in soils and sediments. *Chem Geol* 114:347–363
- Mayes MA, Heal KR, Brandt CC et al (2012) Relation between soil order and sorption of dissolved organic carbon in temperate subsoils. *Soil Sci Soc Am J* 76:1027–1037
- McCarthy JF, Ilavsky J, Jastrow JD et al (2008) Protection of organic carbon in soil microaggregates via restructuring of aggregate porosity and filling of pores with accumulating organic matter. *Geochim Cosmochim Acta* 72:4725–4744
- Melillo JM, Butler S, Johnson J et al (2011) Soil warming, carbon–nitrogen interactions, and forest carbon budgets. *Proc Natl Acad Sci USA* 108:9508–9512
- Moorhead DL, Lashermes G, Sinsabaugh RL (2012) A theoretical model of C- and N-acquiring exoenzyme activities, which balances microbial demands during decomposition. *Soil Biol Biochem* 53:133–141

- Norby RJ, Luo Y (2004) Evaluating ecosystem responses to rising atmospheric CO<sub>2</sub> and global warming in a multi-factor world. *N Phytol* 162:281–293
- O'Brien SL, Jastrow JD (2013) Physical and chemical protection in hierarchical soil aggregates regulates soil carbon and nitrogen recovery in restored perennial grasslands. *Soil Biol Biochem* 61:1–13
- O'Brien SL, Jastrow JD, McFarlane KJ et al (2013) Decadal cycling within long-lived carbon pools revealed by dual isotopic analysis of mineral-associated soil organic matter. *Biogeochemistry* 112:111–125
- Oleson KW, Lawrence DM, Bonan GB et al (2013) Technical description of version 4.5 of the Community Land Model (CLM). NCAR Tech. National Center for Atmospheric Research, Boulder
- Parton WJ, Schimel DS, Cole CV et al (1987) Analysis of factors controlling soil organic matter levels in great plains grasslands. *Soil Sci Soc Am J* 51:1173–1179
- Parton WJ, Scurlock JMO, Ojima DS et al (1995) Impact of climate change on grassland production and soil carbon worldwide. *Glob Change Biol* 1:13–22
- Parton WJ, Hartman M, Ojima D, Schimel D (1998) DAYCENT and its land surface submodel: description and testing. *Glob Planet Change* 19:35–48
- Parton WJ, Hanson PJ, Swanston C et al (2010) ForCent model development and testing using the Enriched Background Isotope Study experiment. *J Geophys Res*. <https://doi.org/10.1029/2009jg001193>
- Paustian K, Parton WJ, Persson J (1992) Modeling soil organic matter in organic-amended and nitrogen-fertilized long-term plots. *Soil Sci Soc Am J* 56:476–488
- Plante AF, Conant RT, Paul EA et al (2006) Acid hydrolysis of easily dispersed and microaggregate-derived silt- and clay-sized fractions to isolate resistant soil organic matter. *Eur J Soil Sci* 57:456–467
- Pronk GJ, Heister K, Ding G-C et al (2012) Development of biogeochemical interfaces in an artificial soil incubation experiment; aggregation and formation of organo-mineral associations. *Geoderma* 189–190:585–594
- Ranjard L, Richaume A (2001) Quantitative and qualitative microscale distribution of bacteria in soil. *Res Microbiol* 152:707–716
- Riley WJ, Maggi F, Kleber M et al (2014) Long residence times of rapidly decomposable soil organic matter: application of a multi-phase, multi-component, and vertically resolved model (BAMS1) to soil carbon dynamics. *Geosci Model Dev* 7:1335–1355
- Rumpel C, Eusterhues K, Kögel-Knabner I (2010) Non-cellulosic neutral sugar contribution to mineral associated organic matter in top- and subsoil horizons of two acid forest soils. *Soil Biol Biochem* 42:379–382
- Schimel DS (1995) Terrestrial ecosystems and the carbon cycle. *Glob Change Biol*. <https://doi.org/10.1111/j.1365-2486.1995.tb00008.x>
- Schimel JP, Weintraub MN (2003) The implications of exoenzyme activity on microbial carbon and nitrogen limitation in soil: a theoretical model. *Soil Biol Biochem* 35:549–563
- Schmidt MWI, Torn MS, Abiven S et al (2011) Persistence of soil organic matter as an ecosystem property. *Nature* 478:49–56
- Segoli M, De Gryze S, Dou F et al (2013) AggModel: a soil organic matter model with measurable pools for use in incubation studies. *Ecol Model* 263:1–9
- Sexstone AJ, Revsbech NP, Parkin TB, Tiedje JM (1985) Direct measurement of oxygen profiles and denitrification rates in soil aggregates. *Soil Sci Soc Am J* 49:645–651
- Sierra CA, Trumbore SE, Davidson EA et al (2012) Predicting decadal trends and transient responses of radiocarbon storage and fluxes in a temperate forest soil. <https://doi.org/10.5194/bg-9-3013-2012>
- Sierra CA, Trumbore SE, Davidson EA et al (2015) Sensitivity of decomposition rates of soil organic matter with respect to simultaneous changes in temperature and moisture. *J Adv Model Earth Syst* 7:335–356
- Sinsabaugh RL, Shah JFF (2012) Ecoenzymatic stoichiometry and ecological theory. *Annu Rev Ecol Evol Syst* 43:313–343
- Sinsabaugh RL, Belnap J, Findlay SG et al (2014a) Extracellular enzyme kinetics scale with resource availability. *Biogeochemistry* 121:287–304
- Sinsabaugh RL, Follstad Shah JJ, Findlay SG et al (2014b) Scaling microbial biomass, metabolism and resource supply. *Biogeochemistry* 122:175–190
- Sinsabaugh RL, Moorhead DL, Xu X, Litvak ME (2017) Plant, microbial and ecosystem carbon use efficiencies interact to stabilize microbial growth as a fraction of gross primary production. *N Phytol*. <https://doi.org/10.1111/nph.14485>
- Sistla SA, Rastetter EB, Schimel JP (2014) Responses of a tundra system to warming using SCAMPS: a stoichiometrically coupled, acclimating microbe–plant–soil model. *Ecol Monogr* 84:151–170
- Six J, Paustian K (2014) Aggregate-associated soil organic matter as an ecosystem property and a measurement tool. *Soil Biol Biochem* 68:A4–A9
- Six J, Elliott ET, Paustian K, Doran JW (1998) Aggregation and soil organic matter accumulation in cultivated and native grassland soils. *Soil Sci Soc Am J* 62:1367–1377
- Six J, Elliott ET, Paustian K (2000) Soil macroaggregate turnover and microaggregate formation: a mechanism for C sequestration under no-tillage agriculture. *Soil Biol Biochem* 32:2099–2103
- Six J, Frey SD, Thiet RK, Batten KM (2006) Bacterial and fungal contributions to carbon sequestration in agroecosystems. *Soil Sci Soc Am J* 70:555
- Smith AP, Bond-Lamberty B, Benschoter BW et al (2017) Shifts in pore connectivity from precipitation versus groundwater rewetting increases soil carbon loss after drought. *Nat Commun*. <https://doi.org/10.1038/s41467-017-01320-x>
- Sollins P, Homann P, Caldwell BA (1996) Stabilization and destabilization of soil organic matter: mechanisms and controls. *Geoderma* 74:65–105
- Sollins P, Kramer MG, Swanston C et al (2009) Sequential density fractionation across soils of contrasting mineralogy: evidence for both microbial- and mineral-controlled soil organic matter stabilization. *Biogeochemistry* 96:209–231
- Steinweg JM, Plante AF, Conant RT et al (2008) Patterns of substrate utilization during long-term incubations at different temperatures. *Soil Biol Biochem* 40:2722–2728
- Sulman BN, Phillips RP, Oishi AC et al (2014) Microbe-driven turnover offsets mineral-mediated storage of soil carbon under elevated CO<sub>2</sub>. *Nat Clim Change* 4:1099–1102

- Suseela V, Conant RT, Wallenstein MD, Dukes JS (2012) Effects of soil moisture on the temperature sensitivity of heterotrophic respiration vary seasonally in an old-field climate change experiment. *Glob Change Biol* 18:336–348
- Tang JY (2015) On the relationships between Michaelis–Menten kinetics, reverse Michaelis–Menten kinetics, Equilibrium Chemistry Approximation kinetics and quadratic kinetics. *Geosci Model Dev Discuss* 8:7663–7691
- Tang J, Riley WJ (2015) Weaker soil carbon–climate feedbacks resulting from microbial and abiotic interactions. *Nat Clim Change*. <https://doi.org/10.1038/nclimate2438>
- Thornton PE, Lamarque J-F, Rosenbloom NA, Mahowald NM (2007) Influence of carbon–nitrogen cycle coupling on land model response to CO<sub>2</sub> fertilization and climate variability. *Glob Biogeochem Cycles*. <https://doi.org/10.1029/2006gb002868>
- Tisdall J, Oades J (1982) Organic matter and water-stable aggregates in soils. *J Soil Sci* 33:141–163
- Todd-Brown KEO, Hopkins FM, Kivlin SN et al (2011) A framework for representing microbial decomposition in coupled climate models. *Biogeochemistry* 109:19–33
- Todd-Brown KEO, Randerson JT, Post WM, et al (2013) Causes of variation in soil carbon simulations from CMIP5 Earth system models and comparison with observations
- Todd-Brown KEO, Randerson JT, Hopkins F et al (2014) Changes in soil organic carbon storage predicted by Earth system models during the 21st century. *Biogeosciences* 11:2341–2356
- Torn MS, Trumbore SE, Chadwick OA, Vitousek PM, Hendricks DM (1997) Mineral control of soil organic carbon storage and turnover. *Nature* 389:170–173
- Torn MS, Swanston CW, Castanha C, Trumbore SE (2009) Storage and turnover of organic matter in soil. In: *Biophysico-chemical processes involving natural nonliving organic matter in environmental systems*. Wiley, Hoboken, p 219–272
- van Ginkel JH, Gorissen A, Polci D (2000) Elevated atmospheric carbon dioxide concentration: effects of increased carbon input in a *Lolium perenne* soil on microorganisms and decomposition. *Soil Biol Biochem* 32:449–456
- Vance ED, Brookes PC, Jenkinson DS (1987) An extraction method for measuring soil microbial biomass C. *Soil Biol Biochem* 19:703–707
- Virto I, Barré P, Chenu C (2008) Microaggregation and organic matter storage at the silt-size scale. *Geoderma* 146:326–335
- von Lützow M, Kögel-Knabner I, Ekschmitt K et al (2007) SOM fractionation methods: relevance to functional pools and to stabilization mechanisms. *Soil Biol Biochem* 39:2183–2207
- Wang G, Post WM, Mayes MA (2013) Development of microbial-enzyme-mediated decomposition model parameters through steady-state and dynamic analyses. *Ecol Appl* 23:255–272
- Wang YP, Jiang J, Chen-Charpentier B et al (2016) Responses of two nonlinear microbial models to warming and increased carbon input. *Biogeosciences* 13:887–902
- Wershaw RL (1986) A new model for humic materials and their interactions with hydrophobic organic chemicals in soil–water or sediment–water systems. *J Contam Hydrol* 1:29–45
- Wieder WR, Bonan GB, Allison SD (2013) Global soil carbon projections are improved by modelling microbial processes. *Nat Clim Change* 3:1–7
- Wieder WR, Grandy AS, Kallenbach CM, Bonan GB (2014) Integrating microbial physiology and physio-chemical principles in soils with the Microbial-MIneral Carbon Stabilization (MIMICS) model. *Biogeosciences* 11:3899–3917
- Wieder WR, Allison SD, Davidson EA et al (2015a) Explicitly representing soil microbial processes in Earth system models. *Glob Biogeochem Cycles* 29:1782–1800
- Wieder WR, Grandy AS, Kallenbach CM et al (2015b) Representing life in the Earth system with soil microbial functional traits in the MIMICS model. *Geosci Model Dev Discuss* 8:2011–2052
- Xu X, Schimel JP, Thornton PE et al (2014) Substrate and environmental controls on microbial assimilation of soil organic carbon: a framework for Earth system models. *Ecol Lett* 17:547–555
- Young IM, Crawford JW (2004) Interactions and self-organization in the soil–microbe complex. *Science* 304:1634–1637
- Young IM, Crawford JW, Nunan N, et al (2008) Chapter 4 Microbial Distribution in Soils: Physics and Scaling. In: *Advances in Agronomy*. Academic Press, pp 81–121
- Zaehle S, Medlyn BE, De Kauwe MG et al (2014) Evaluation of 11 terrestrial carbon–nitrogen cycle models against observations from two temperate Free-Air CO<sub>2</sub> Enrichment studies. *N Phytol* 202:803–822
- Zhuang J, McCarthy JF, Perfect E et al (2008) Soil water hysteresis in water-stable microaggregates as affected by organic matter. *Soil Sci Soc Am J* 72:212–220